

Buckling Load Reduction for Stiffened Panels Due to Cutouts in Ribs

Andrew Watson,* Fred W. Williams,† and David Kennedy‡
University of Wales, Cardiff CF2 3TB, Wales, United Kingdom

In aerospace structures it is common to find stiffened panels with transverse supporting structures, e.g., wing ribs or fuselage frames. Incorporating cutouts into these supporting structures to allow the stringers to pass through freely considerably reduces the buckling load of the panels. It is shown that a minor modification in the fabrication of the stiffened panel gives most of the advantages of cutouts while still giving a buckling load close to that of a panel with no cutouts.

Introduction

IN aerospace structures it is common to find stiffened panels with transverse supporting structures, e.g., wing ribs or fuselage frames. The aim of this parametric study is to see whether cutouts in these transverse supporting structures, through which stringers pass, reduce the buckling loads or, alternatively, increase the mass when designing. It is shown that incorporating such cutouts into the transverse supporting structure can considerably reduce the buckling load of the panel. This is done by considering the limiting case of supporting structures that completely clamp the ends of the panel except where the cutouts are.

The results are compared with those for a panel with completely clamped ends, i.e., without cutouts. The reduction in the buckling capacity is due to the lack of constraints within each cutout allowing the buckling mode to pass through it to the next bay. The presence of the cutouts means that the buckling mode does not have to repeat in every bay, unlike the case without cutouts.

Modeling of Clamped Ends

All computing is performed using VIPASA with constraints and optimization (VICONOPT) (Ref. 1), which is a Fortran 77 computer program that incorporates the earlier programs VIPASA (vibration and instability of plate assemblies including shear and anisotropy)² and VIPASA with constraints (VICON) (Ref. 3). It covers any prismatic plate assembly, i.e., panels of constant cross section, composed of anisotropic plates each of which can carry any combination of longitudinally invariant in-plane stresses. It can be used as either an analysis or an optimum design program. The VIPASA and VICON analysis features cover the calculation of eigenvalues, i.e., the critical load factors in elastic buckling problems or the natural frequencies in undamped vibration problems. The analysis is based upon the exact solution of the governing differential equations of the constituent members, yielding exact stiffness matrices of which the elements are transcendental functions of the load factor or frequency. The resulting transcendental eigenproblem requires an iterative solution that is performed using the Wittrick-Williams algorithm.⁴

VICON can be used to solve any analysis problem that could otherwise be solved by VIPASA but includes substantial additional capability as well, because VIPASA assumes modes with sinusoidal longitudinal variation of half wavelength λ , whereas VICON modes are weighted sums of such modes for a series of values of λ .

Displacements along the infinite length of the plate assembly, of which a typical plate is shown in Fig. 1, are assumed to be the real vector D_A given by

$$D_A = \sum_{m=-\infty}^{\infty} D_m \exp(2i\pi mx/L) \quad (1)$$

where L is the length over which the mode repeats, D_m is a complex displacement amplitude vector for the assumed sinusoidal longitudinal half wavelength λ , and m is the number of sinusoidal waves in length L , so that $\lambda = L/2m$.

VICONOPT uses Lagrangian multipliers to couple the responses for an appropriate³ set of the half wavelengths λ of the infinitely long plate assembly so as to satisfy support conditions repeating at longitudinal intervals l . Thus a plate assembly of finite length l with simply supported ends may be modeled reasonably accurately by representing the (continuous) transverse simple supports by a line of rigid point supports at $x = 0$. The results assume that the mode repeats over a length $L = 2l/\xi$ for some value $0 \leq \xi \leq 1$. Each value of ξ generates the truncated infinite series

$$\lambda = l/(\xi + 2m) \quad (m = 0, \pm 1, \pm 2, \pm 3, \pm 4, \dots, \pm q) \quad (2)$$

where q is chosen to be high enough to give acceptable results. Table 1 lists the values of λ derived from Eq. (2) for typical values of ξ , with negative values indicating the use of complex conjugate matrices and ∞ indicating a rigid-body mode.³

An appropriate model of a clamped endpoint support at $x = 0$ for the j th element D_{Aj} of D_A requires, if the j th element is a w displacement (see Fig. 1), that w and $dw/dx = 0$. After differentiating Eq. (1), this gives the constraints as

$$\sum D_{mj} = 0 \quad (3)$$

$$\sum m D_{mj} = 0 \quad (4)$$

Modeling of the Cutouts

To model the cutouts in the transverse supporting structure shown in Fig. 2, which repeats at longitudinal intervals of l , it is assumed that the supporting structure is very stiff and behaves as a clamped support in the limiting case. So in the problem without cutouts the complete transverse edges of both the skin and stiffeners were modeled as clamped when using VICONOPT, whereas in the problem with cutouts all constraints were removed from the stiffener and from the portions of skin lying within the cutouts.

Figure 3a denotes by crosses the nodes at which point supports were present when there were no cutouts. These nodes were equally spaced for all plates of the assembly. It was found that excellent results could be obtained without the expense of constraining all of $u, v, w, dw/dx, dv/dx$, and dw/dy at constrained nodes. Hence Table 2 shows the constraints used, for the cases with and without cutouts, referred to the global axis system shown in Fig. 3a. The panel was aluminum, subjected to a compressive axial force

Received March 19, 1997; revision received July 30, 1997; accepted for publication Sept. 22, 1997. Copyright © 1997 by the American Institute of Aeronautics and Astronautics, Inc. All rights reserved.

*Research Student, Division of Structural Engineering, Cardiff School of Engineering, Queen's Buildings, The Parade, P.O. Box 686.

†Professor, Head of Structures, Division of Structural Engineering, Cardiff School of Engineering, Queen's Buildings, The Parade, P.O. Box 686. Member AIAA.

‡Lecturer, Division of Structural Engineering, Cardiff School of Engineering, Queen's Buildings, The Parade, P.O. Box 686. Member AIAA.

Table 1 Half wavelengths λ used in analysis³

ξ	λ
0	$\infty, l/2, l/4, l/6, l/8, \dots$
0.25	$4l, -4l/7, 4l/9, -4l/15, 4l/17, \dots$
0.5	$2l, -2l/3, 2l/5, -2l/7, 2l/9, \dots$
0.75	$4l/3, -4l/5, 4l/11, -4l/13, 4l/19, \dots$
1	$l, l/3, l/5, l/7, l/9, \dots$

Table 2 Degrees of freedom constrained at each node for $\xi = 1$

	With cutouts	Without cutouts
Flange nodes	—	$u, dw/dx, dv/dx$
Web only nodes	—	$u, dw/dx$
Skin	$u, w, dw/dx, dv/dx$	$u, w, dw/dx, dv/dx$

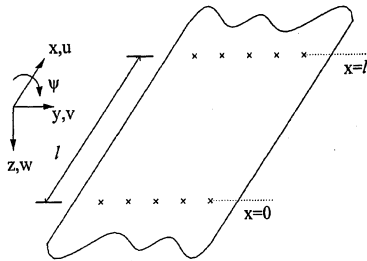


Fig. 1 Plate, showing axis and displacement systems. Crosses denote nodes needed when rigid point supports are used.

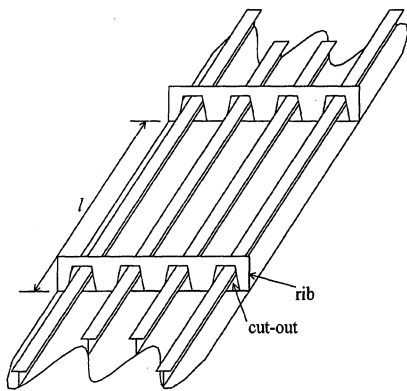
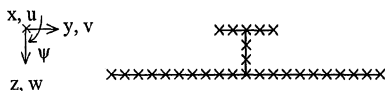
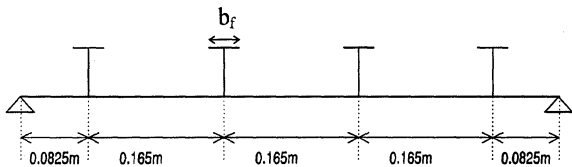


Fig. 2 Panel with ribs and cutouts.



a) Typical T stiffener and associated skin, with the (evenly spaced) crosses denoting nodes at which point supports are present



b) Complete panel, approximately to scale and with Δ denoting a continuous line support that enforces $w = 0$

Fig. 3 Cross section of panel studied.

of 1.16 MN, had $l = 1.98$ m, and had four T stiffeners spaced as shown on the cross-section view of Fig. 3b.

The panel was first optimized by using VICONOPT to make the local and overall buckling modes for $l = 1.8$ m coincident. This optimization was performed without cutouts, using the constraints of Table 2 with approximately 50% of the nodes shown in Fig. 3a. The optimized values of the design variables were stiffener height between skin and flange centerlines = 54.20 mm and thicknesses = 5.06 and 3.10 mm for the skin and flanges, respectively. The flange breadth (b_f , see Fig. 3) was held constant at 30 mm, and the web thickness was constrained to equal half the skin thickness. Offsets²

were used to improve the modeling of the structure. The length of this optimized panel was then increased by 10%, i.e., to make l have the correct value of 1.98 m. This procedure ensured that overall buckling governed failure.

Results

Table 3 shows the decrease in the buckling load factor caused by introducing cutouts. The results shown are for $\xi = 1.0$ because $\xi = 1.0$ gave lower results than any other $\xi (0 \leq \xi < 1.0)$ and are for cutout widths equal to 0, 20, 40, and 60% of the stiffener pitch.

The load factors given in Table 3 are converged values obtained by curve extrapolation, i.e., best fit quadratic curves, using the points on the plots of load factor against $1/q^2$ shown in Fig. 4. The results of the quadratic extrapolation are shown on the zero abscissa of Fig. 4. The intercept on the vertical axis is taken as the required load factor because it corresponds to an infinite number of half wavelengths being used. The dashed-straight-line extrapolations shown in Fig. 4 can be seen to give predictions close to the results of Table 3.

Figure 5 shows $\xi = 1$ results for the case with 60% cutouts and a single additional constraint on each stiffener that prevents u

Table 3 Load factors with and without cutouts

Without cutouts	Cutout width as % of stiffener pitch			
	0	20	40	60
0.838 (0.841)	0.418	0.392	0.379	0.369

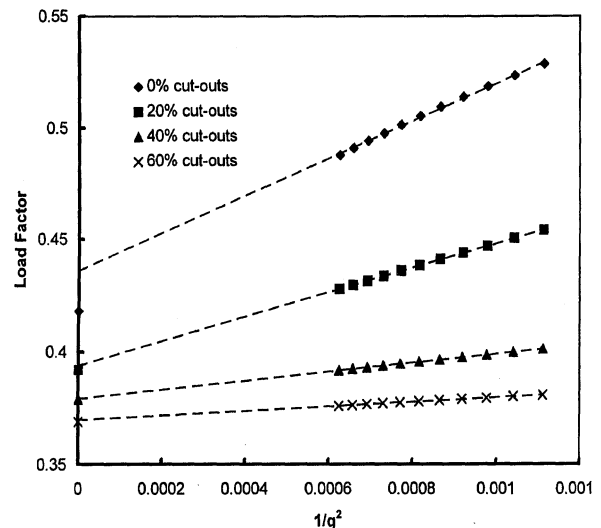


Fig. 4 Graph showing convergence for different sized cutouts, with results of quadratic convergence shown on zero abscissa.

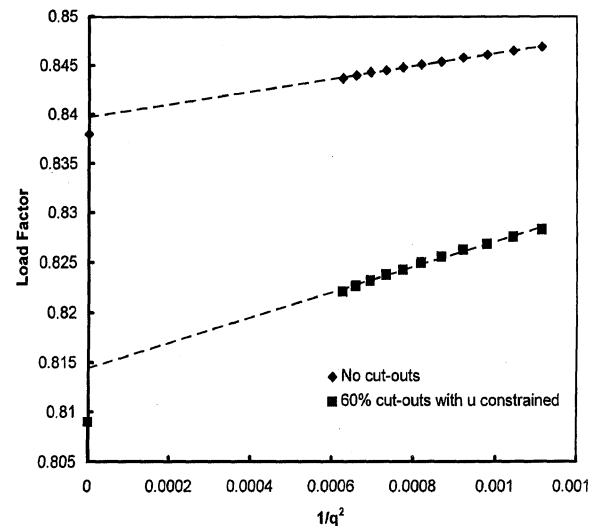


Fig. 5 Effect of constraining u at flange/web junctions compared with case without cutouts, with results of quadratic convergence shown on zero abscissa.

displacement at the web/flange junction and also for the case without cutouts. The best fit quadratic curve extrapolations, shown on the zero abscissa, gave load factors slightly below those of the linear extrapolations shown as dashed lines in Fig. 5, the quadratic extrapolations being 0.838, i.e., the result of Table 3, for the case without cutouts and 0.809 for the 60% cutouts case. The introduction of the u constraint causes a large increase in the load factor, i.e., from 0.369 to 0.809, so that it becomes close to the result for the case without cutouts, i.e., 0.838.

It can be shown that, for the case with no cutouts, results for $\xi = 0.0$ converge on the clamped result as q is increased much more quickly than do the $\xi = 1$ results. Therefore the converged $\xi = 0$ result is shown in brackets in Table 3, from which it can be seen that the $\xi = 1$ result of 0.838 extrapolated from Fig. 5 is very accurate, which gives confidence in the other extrapolations of Figs. 4 and 5.

VICONOPT solutions have been validated against finite element-based methods for shear loaded panels with simply supported ends.⁵ A paper giving solutions for fully clamped ended plates that have been validated against the results of Roark⁶ will shortly be submitted for publication.

Conclusions

The results clearly show that the presence of a cutout significantly reduces the buckling load of a panel. However, the result for the 0% cutout, i.e., where the stiffener attachment point is still constrained but all of its other points are free, also shows a significant decrease. This is due to the transverse line support behaving more like a simple support than a true clamped support. So, irrespective of the size of the cutout, leaving the stiffener unconstrained causes the buckling load to drop significantly.

The cutout results of Fig. 5 clearly show a major increase compared with Fig. 4, with the load factor being quite close to that for the fully clamped case. This has important implications for the fabrication of stiffened panels with transverse supporting structures, namely, that it is very beneficial to add to each stiffener web simple extra bracing to prevent displacement in the longitudinal direction

at the edge remote from the skin. This gives most of the fabrication advantages of having cutouts while still giving a buckling load close to that of a panel with no cutouts.

The results presented are only for a metal panel with T stiffeners, but the conclusions are likely to be more generally applicable and can be checked for any given panel by using software such as that used herein.

Acknowledgments

The first author gratefully acknowledges financial support from the Engineering and Physical Sciences Research Council and British Aerospace.

References

- ¹Butler, R., and Williams, F. W., "Optimum Design Using VICONOPT, a Buckling and Strength Constraint Program for Prismatic Assemblies of Anisotropic Plates," *Computers and Structures*, Vol. 43, No. 4, 1992, pp. 699-708.
- ²Wittrick, W. H., and Williams, F. W., "Buckling and Vibration of Anisotropic or Isotropic Plate Assemblies Under Combined Loadings," *International Journal of Mechanical Sciences*, Vol. 16, No. 4, 1974, pp. 209-239.
- ³Anderson, M. S., Williams, F. W., and Wright, C. J., "Buckling and Vibration of Any Prismatic Assembly of Shear and Compression Loaded Anisotropic Plates with an Arbitrary Supporting Structure," *International Journal of Mechanical Sciences*, Vol. 25, No. 8, 1983, pp. 585-596.
- ⁴Wittrick, W. H., and Williams, F. W., "A General Algorithm for Computing Natural Frequencies of Elastic Structures," *Quarterly Journal of Mechanics and Applied Mathematics*, Vol. 24, Pt. 3, 1971, pp. 263-284.
- ⁵Kennedy, D., Williams, F. W., and Anderson, M. S., "Buckling and Vibration Analysis of Laminated Panels Using VICONOPT," *Journal of Aerospace Engineering, American Society of Civil Engineers*, Vol. 7, No. 3, 1994, pp. 245-262.
- ⁶Young, W. C., *Roark's Formulas for Stress and Strain*, 6th ed., McGraw-Hill, New York, 1989, pp. 684-686.

A. D. Belegundu
Associate Editor